Geodinamica Acta 14 (2001) 1–17

S0985311100010536/FLA

Neotectonic and volcanic characteristics of the Karasu fault zone (Anatolia, Turkey): The transition zone between the Dead Sea transform and the East Anatolian fault zone

Bora Rojay[a]*, Ariel Heimann[b], Vedat Toprak[a]

[a] Department of Geological Engineering, Middle East Technical University, 06531 Ankara, Turkey
[b] Geological Survey of Israel, 30 Malkhe Israel St., Jerusalem, 95501, Israel

Received 2 January 2000; accepted 21 May 2000

Abstract – The Karasu Rift (Antakya province, SE Turkey) has developed between east-dipping, NNE-striking faults of the Karasu fault zone, which define the western margin of the rift and west-dipping, N–S to N20–30E-striking faults of Dead Sea Transform fault zone (DST) in the central part and eastern margin of the rift. The strand of the Karasu fault zone that bounds the basin from west forms a linkage zone between DST and East Anatolian fault zone (EAFZ). The greater vertical offset on the western margin faults relative to the eastern ones indicates asymmetrical evolution of the rift as implied by the higher escarpments and accumulation of extensive, thick alluvial fans on the western margins of the rift. The thickness of the Quaternary sedimentary fill is more than 465 m, with clastic sediments intercalated with basaltic lavas. The Quaternary alkali basaltic volcanism accompanied fluvial to lacustrine sedimentation between 1.57 ± 0.08 and 0.05 ± 0.03 Ma. The faults are left-lateral oblique-slip faults as indicated by left-stepping faulting patterns, slip-lineation data and left-laterally offset lava flows and stream channels along the Karasu fault zone. At Hacılar village, an offset lava flow, dated to 0.08 ± 0.06 Ma, indicates a rate of left-lateral oblique slip of approximately 4.1 mm·year^{-1}. Overall, the Karasu Rift is an asymmetrical transtensional basin, which has developed between seismically active splays of the left-lateral DST and the left-lateral oblique-slip Karasu fault zone during the neotectonic period. © 2001 Éditions scientifiques et médicales Elsevier SAS

continental alkali basaltic volcanism / Karasu fault zone / Karasu Rift / Dead Sea transform fault / Anatolia / Turkey

*Correspondence and reprints.
E-mail address: brojay@metu.edu.tr (B. Rojay).

1. Introduction

The relative motion between the Arabian, African and Eurasian plates is the key for the geodynamics of the Eastern Mediterranean region. The motion of the African and Arabian plates towards the Eurasian Plate has caused convergence in the Eastern Mediterranean region since the Late Cretaceous (*figure 1*) [1–5].

As a result of this collision between the Arabian and the Eurasian plates, the Anatolian block has migrated westward towards the Eastern Mediterranean Ridge on the African Plate (*figure 1*). This lateral extrusion of the Anatolian block is accommodated by two major continental transform faults: – the North Anatolian fault zone (NAFZ) and the East Anatolian fault zone (EAFZ) [e.g., 1, 5–8].

The EAFZ and the Dead Sea transform fault zone (DST) meet at a triple junction between the Arabian Plate, the African Plate and the Anatolian Block. The nature of slip on the DST, the bounding fault between the Arabian and African plates [e.g. 9, 10], and the EAFZ, are individually well resolved, based on field, geophysical and kinematic data. However, the nature and geometry at their continuations as they approach the triple junction are still discussed.

The DST is a dominantly left-lateral transform fault, with an extensional component, that forms various rift depressions [11–14]. It is more than 1 000 km long, links the Red Sea, where oceanic spreading takes place, to the Taurus zone of plate collision (*figure 1*). It became active in Middle Miocene time and it is still seismically active [e.g., 14].

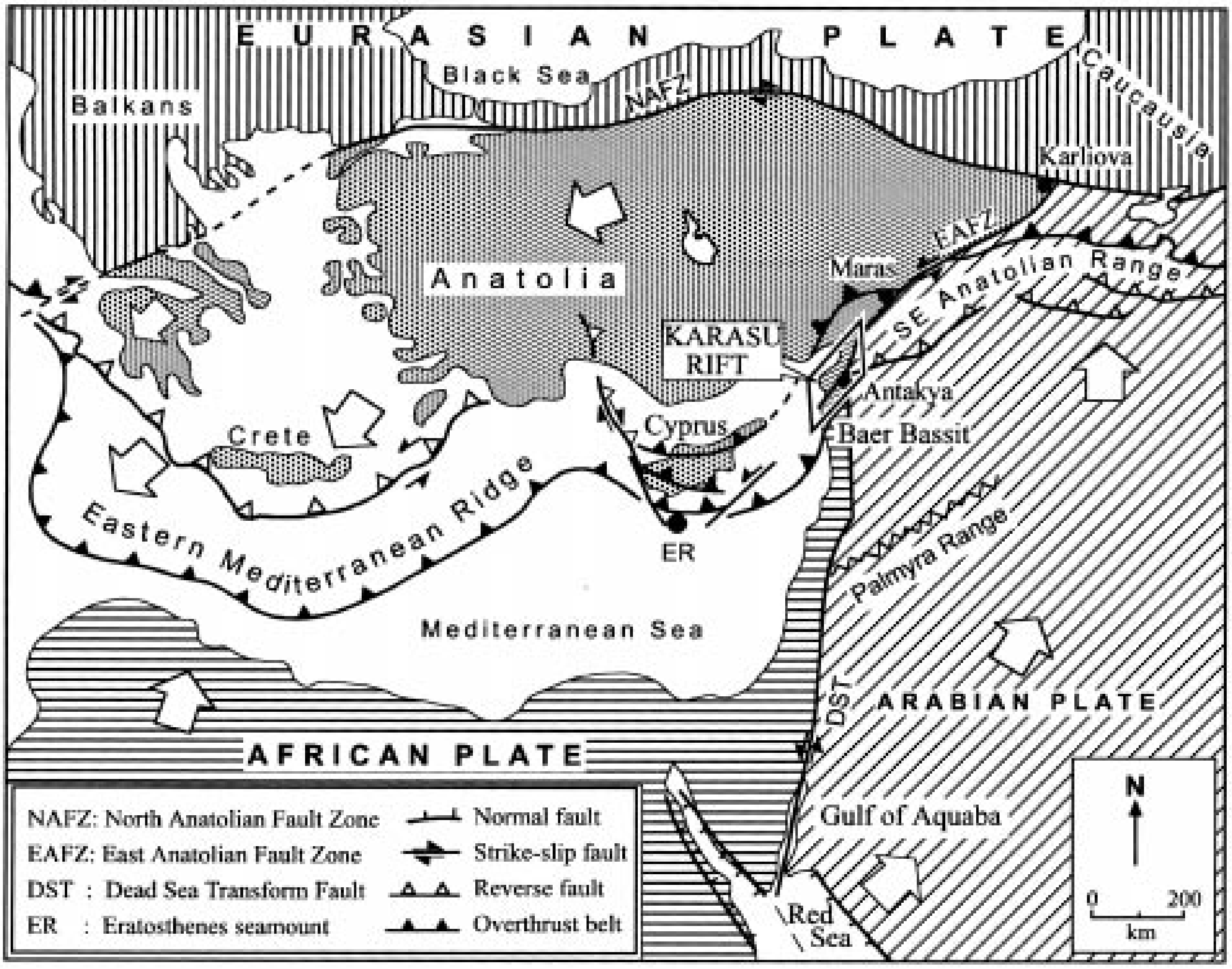

Figure 1. Major neotectonic elements of Eastern Mediterranean. Arrows show direction of plate motions. (Simplified and modified from [48–51]).

An maximum offset of 105–107 km was measured in the section connecting Mt. Hermon in Lebanon (Yammunneh fault) and the Gulf of Aqaba [e.g. 12, 15]. Lateral offset of the DST to the north of the Yammunneh fault is much less constrained. A 70–80 km of displacement was suggested by displaced Upper Cretaceous ophiolites in northern Syria and southeastern Turkey where the attitudes of ophiolitic units are unknown to northern tip of DST [16]. However, only 10–20 km of total slip was also suggested for that section [e.g., 17].

The EAFZ has an average trend of N66°E and displays a left-lateral strike-slip character with various restraining bends. It is located between Karliova (eastern Anatolia) where it joins the NAFZ and Türkoğlu (south of Maraş) [1, 8, 18–23]. The measured slip on the EAFZ is about 3.5–13 km on displaced Euphrates River channels and 15–27 km on displaced pre-Pliocene units [4, 18, 19, 22]. However these estimates of the displacement on the EAFZ are much too low according to Westaway and Arger (1996) [24] who propose an offset of 35–40 km.

In addition to geological and kinematic estimates for the displacements, fault plane solutions of earthquakes clearly show dextral slip sense along the NAFZ and sinistral slip senses along the EAFZ and DST [25, 26]. It is evident that the region is seismically active.

A comprehensive slip lineation analyses of fault surfaces concluded that two phases of deformation occurred in the area; an older N–S directed compressional phase and a more recent E–W extensional phase [27, 28].

The direct relations between the DST and the EAFZ are a matter of debate due to lack of data from this tectonically complicated area (S of Maraş). Various views are proposed; a) the EAFZ continues in southwestern trend from Karliova to north of Cyprus and is not directly connected to the DST [4, 24, 27, 29]; b) The Türkoğlu–Amik segment (Karasu fault zone) is interpreted as a separate fault [28–31], c) the EAFZ continues until Samandağ (Mediterranean Sea) in splay or left-stepping pattern [8, 22, 23, 27, 29, 32], and finally, d) the EAFZ interpreted as a northward continuation of the DST [18, 20].

The Karasu Rift is located within the EAFZ and the DST. Any interpretation, as discussed above, can relate the formation of this rift to the DST, to the EAFZ, to a combination of them, or as a transition zone between them. The rift has been interpreted as a pull-apart basin [30, 32, 33], as a half-graben caused by a flexural bend [23], as a graben resulting from divergent strike-slip motion [20, 29, 32, 34], as a graben resulting from the westward escape of the Anatolian Plate [28].

The Maraş–Antakya–İskenderun region is located within a seismically active region with significant activity since historical times [35]. Most of the largest known historic earthquakes occurred in the Antakya region [35]. The most recent earthquake (January 22, 1997, with M = 5.5; [36]) occurred to the west of Antakya. It is thus evident that the rift is seismically active. This earthquake's fault plane solution indicates a NE–SW left-lateral fault plane with a normal dip-slip component [36].

The aim of this paper is to shed some light onto the neotectonic evolution of the Karasu Rift based on K-Ar dating of its volcanism, age and type of faulting during the Plio-Quaternary period.

2. Geological setting of the Karasu Rift

The NNE–SSW-trending Karasu Rift is situated between Maraş and Antakya in southern Turkey (*figure 2*). It is about 150 km long and 10–25 km wide, being separated into two sub basins by a saddle between Türkoğlu and Fevzipaşa (*figure 2*). The valley is surrounded by uplifted mountain ranges on all sides. The Amanos Mountains to the west are composed of Pre-Cambrian to Eocene rock units; the SE Anatolian mountain range to the east is made of Cretaceous to Miocene rock units; and the Baer–Bassit range to the south is pre-dominantly composed of Cretaceous ophiolite and Miocene rock units. The Karasu Rift is bounded between two fault systems: the NNE-striking fault system which defines the western margin of the rift, and the N–S to N20°–30°E-striking faults on its eastern margin and in its central part (*figures 2* and *3*). The northern end of this fault system seems to combine with the EAFZ in the area between Türkoğlu and Pazarcık (S and SE of Maraş). The southern end of the Karasu fault system splays out into the N40°E-trending Antakya–Samandağ segment and the N–S-trending Asi River segment that are the northern continuation of the DST in Anatolia (*figure 2*). The WNW-trending oblique-slip faults control the southern boundary of the Karasu Rift where the Amik Plain has subsided (*figure 2*).

The Karasu Rift was developed on pre-Pliocene basement consisting of two rock series: Paleozoic crustal units with a Mesozoic allochthonous ophiolitic complex [37], and a 1 300 m thick, folded Upper Miocene–Lower Pliocene (?) sequence [32]. Plio-Quaternary sediments and Quaternary volcanics unconformably overlie the deformed and folded Miocene beds.

The N–S-to NNE-trending tectonically complicated Karasu Rift is thus characterised by active faulting, basaltic volcanism, and sedimentation during the Quaternary.

3. Quaternary volcanism of the Karasu fault

3.1. Extent and composition of the volcanic field

The Quaternary basaltic volcanics are confined to a limited section of the rift between Kırıkhan, Reyhanlı and Fevzipaşa. They form a belt covering an area, which is 94 km long and 12–25 km wide (*figures 2* and *4*). Spatial distribution of these volcanics within the rift is revealed by borehole data (*table I, figure 4*). Accordingly, the volcanic field is confined to the northern part and flanks of the rift.

Volcanic rocks within the rift are composed of several distinct lavas, which are easily distinguished in the field and in aerial photographs. Eruption centres of most of the lavas are located at both margins of the rift, where secondary faults adjoin master faults, between step-over, and on the rift shoulders (*figures 3*and *5*). These eruption centres are morphologically well preserved, elevated cinder cones.

In most cases, these lavas filled pre-existing Quaternary valleys: some of them are intercalated with Quaternary fluvial deposits (*figure 4*). In three wells (boreholes 472, 2632 and 479) three distinct basaltic lavas were penetrated with a maximum total observable thickness of more than 122 m (borehole 472) (*table I, figure 4*).

The northern and southern limits of the volcanic field are estimated by the presence or absence of the basaltic lavas in boreholes to the NE of Fevzipaşa and to the north of Amik Lake (*figure 4*).

The volcanics have been classified as quartz tholeiites, olivine tholeiites, and alkali olivine basalts, most probably from a single magma source, with 46–52 % SiO_2 and 3.5–4.9 % total alkalis, and limited crustal contamination [28, 33, 38, 39].

3.2. Radiometric dating

Radiometric dating of the basaltic lavas of the Karasu Rift has previously determined an age span of 2.10 to 0.35 Ma (*table III*) [33]. Nevertheless, field observations show some

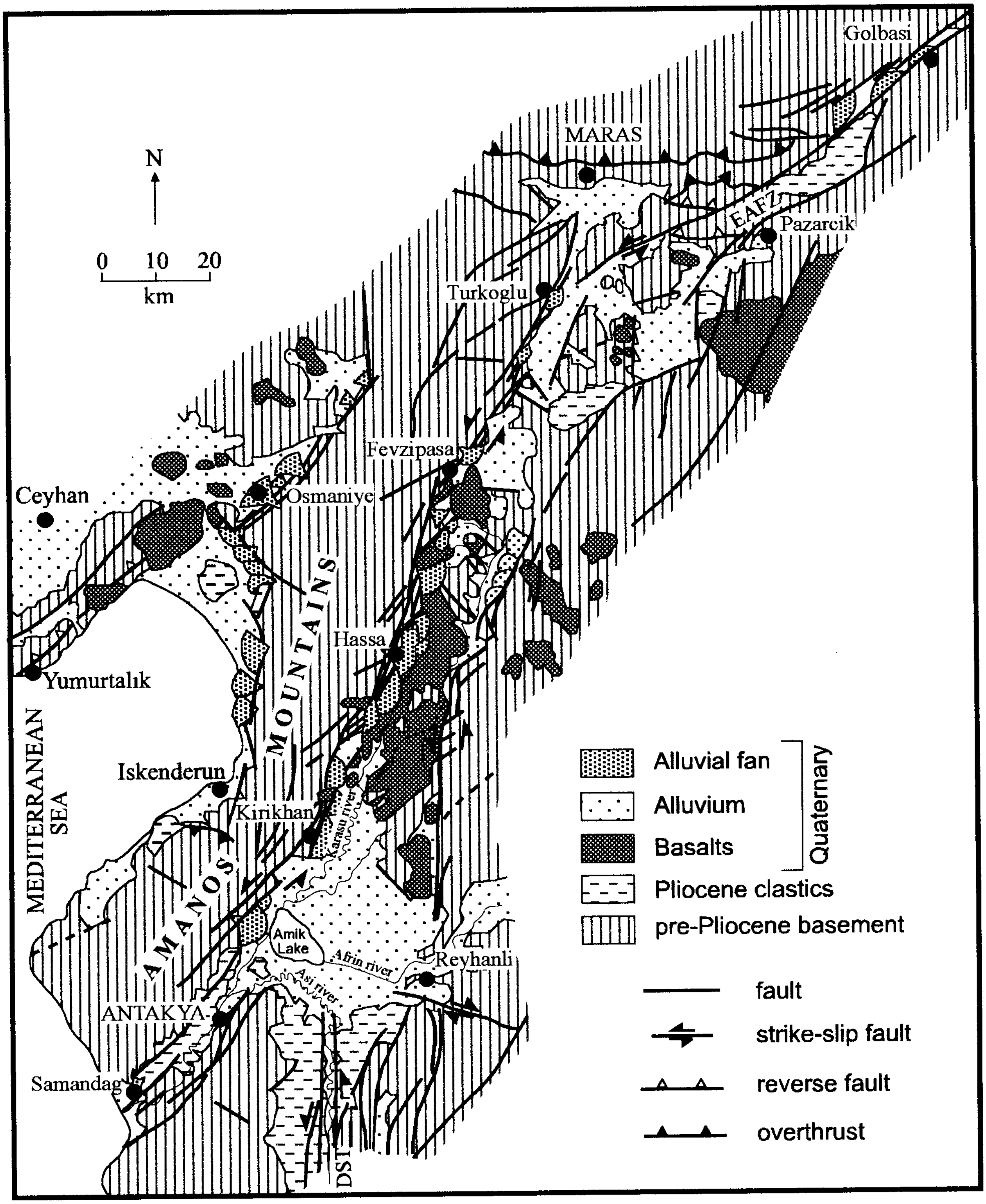

Figure 2. Regional geological map of the Karasu Rift and its vicinity (simplified from 1:500 000 scale geological map of Turkey [52] and modified by aerial photo analysis). DST: Dead Sea transform fault zone (continuation of Gharb segment), EAFZ: East Anatolian fault zone.

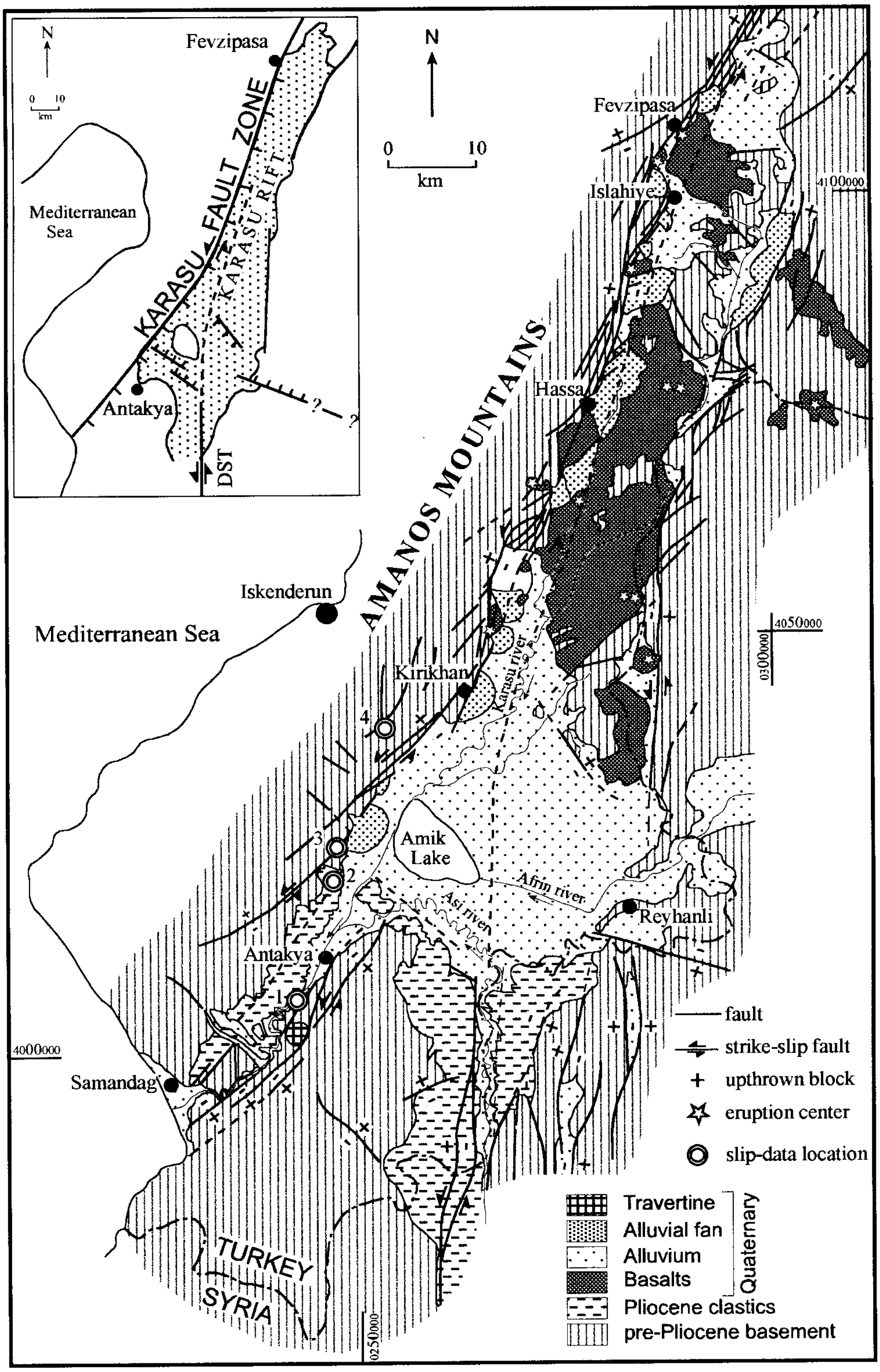

Figure 3. Geological map of Karasu Rift. DST: Dead Sea transform fault zone (continuation of Gharb segment). Inset map shows the major neotectonic elements of the Karasu Rift.

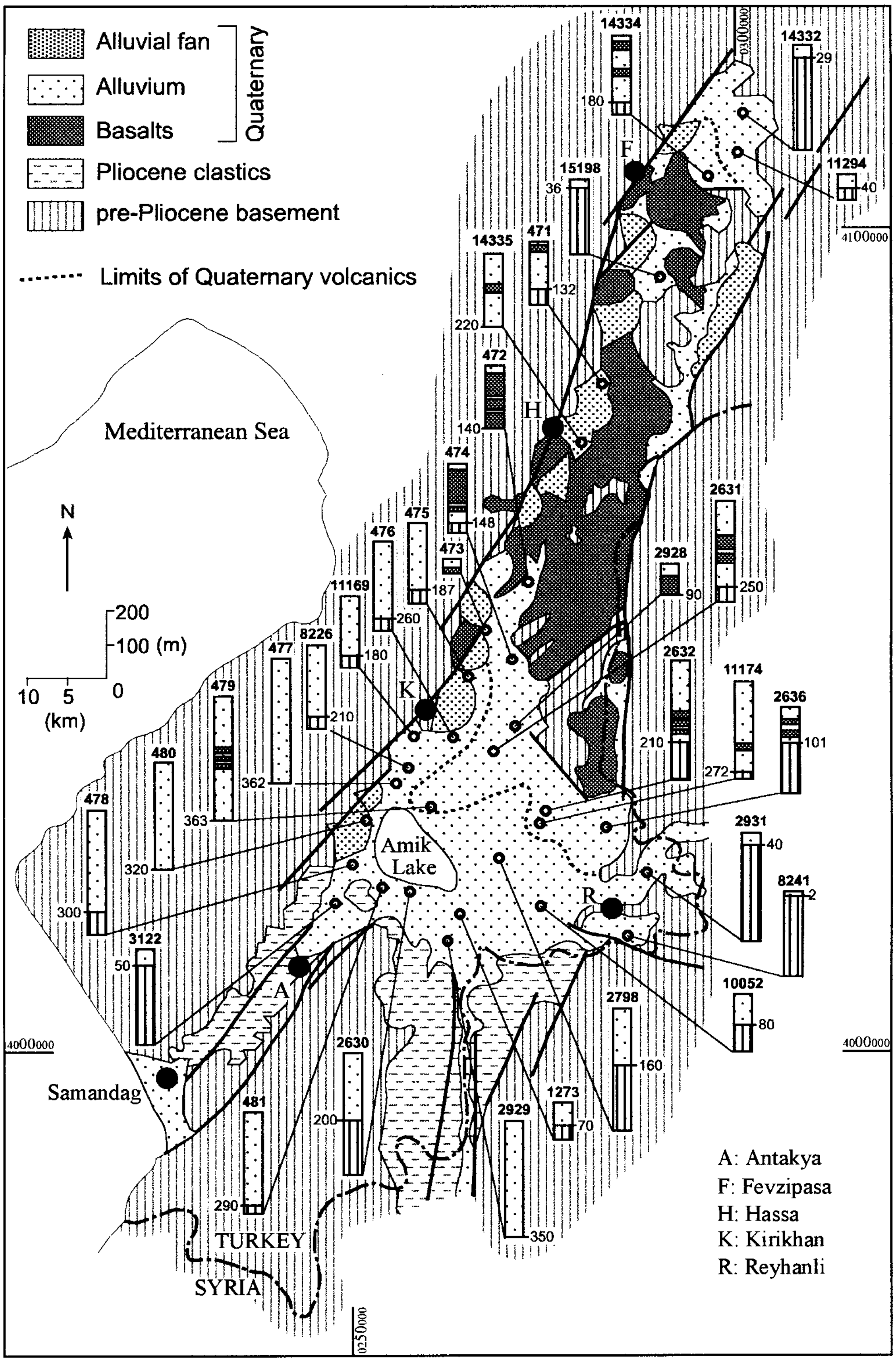

Figure 4. Borehole data from Karasu Rift. Number on top of sections refers to borehole number; number at side of the section refers to the depth (*table I*). Note that the stratigraphy is simplified in the sections into three units as: pre-Pliocene basement rocks, Quaternary sedimentary units and Quaternary basaltic rocks intercalated with sediments (Borehole data are from [42])

Table I. Borehole data for Karasu Rift (DSİ [42]).

Well	UTM-X Coor.	UTM-Y Coor.	Elevation (m)	Total Depth (m) (1)	Frequency of lavas (2)	Thickness of lavas (m) (3)
471	284470	4081490	392.5	140	1	9
472	272580	4056490	130.00	137	3	121
473	268630	4051760	109.14	35	1	11
474	271810	4046975	87.48	151	2	109
475	265300	4044410	97.17	190		
476	262470	4038670	85.65	250		
477	255840	4032860	90.00	362		
478	250955	4022180	87.36	356		
479	263530	4031755	83.74	363	3	56
480	252880	4028270	87.59	309		
481	255350	4022790	79.89	300		
1273	265940	4016620	85.19	100		
2630	257025	4022025	81.67	360		
2631	267960	4035940	82.10	356	2	59
2632	273730	4030075	86.34	350	3	63
2636	280470	4024650	94.66	250	2	30
2798	272425	4023340	86.40	356		
2928	272290	4039810	84.00	93	1	62
2929	263175	4012755	89.00	350		
2931	286640	4020550	125.37	318		
3122	248840	4018420	90.00	283		
8226	257240	4036465	104.58	223		
8241	282590	4013310	183.50	238		
10052	275425	4017125	950.00	160		
11169	259890	4038675	100.00	210		
11174	273970	4028305	89.00	290		
11294	300124	4108050	484	50		
14332	301650	4113625	477.50	247		
14334	298925	4106670	482.05	202	2	41
14335	281575	4074610	342.5	225	1	10
15198	289550	4094050	447.5	195		

(1) Thickness of the borehole
(2) Number of individual lava flows interfingered with clastic layers
(3) Total thickness of all lava flows

different stratigraphic relations with previous age determinations, which suggest that at least some of the lavas are very young. This is true for several lavas, especially for the flow unit located south of Köroğlu, which was dated as 2.10 Ma by Çapan et al [33]. The freshness and the morphology of the lavas as well as their stratigraphic relations with Quaternary sediments suggest that they are of Quaternary age. Therefore, re-sampling and dating of the volcanic field were carried out in the same field (*figure 5*).

Unfortunately, two other volcanic centres (on the Syrian border, *figure 5*) could not be sampled and dated.

3.3. K-Ar Method

A short description of the experimental procedures used is as follows [40, 41]. Samples of approximately 1 kg were collected from each site. Special care was taken in choosing fresh samples. Only samples which showed none (to very minimum) alteration were dated. Each sample was crushed and sieved (70-90 mesh) and washed with water, alcohol, and acetone 0.5 M HCl was used for leaching the samples for one hour. Final cleaning of the samples was carried out by magnetic separation. Potassium was measured by atomic absorption and ^{40}Ar by isotope dilution. Ar was analysed on a VG MM-1200B mass spectrometer at the Geological Survey of Israel Geochronological laboratory.

3.4. Results on Quaternary volcanism

The results of the analysis are given in *table II* and *III* and will be discussed according to its geographical distribution from south to north.

Two lavas in the vicinity of Ceylanlı were dated to 0.66 ± 0.04 and 1.57 ± 0.08 Ma (Sites 1, 2 respectively, *table II*, *figure 5*). These lavas are part of a relatively old volcanic activity in the area. The 1.57 Ma lava is faulted by one of

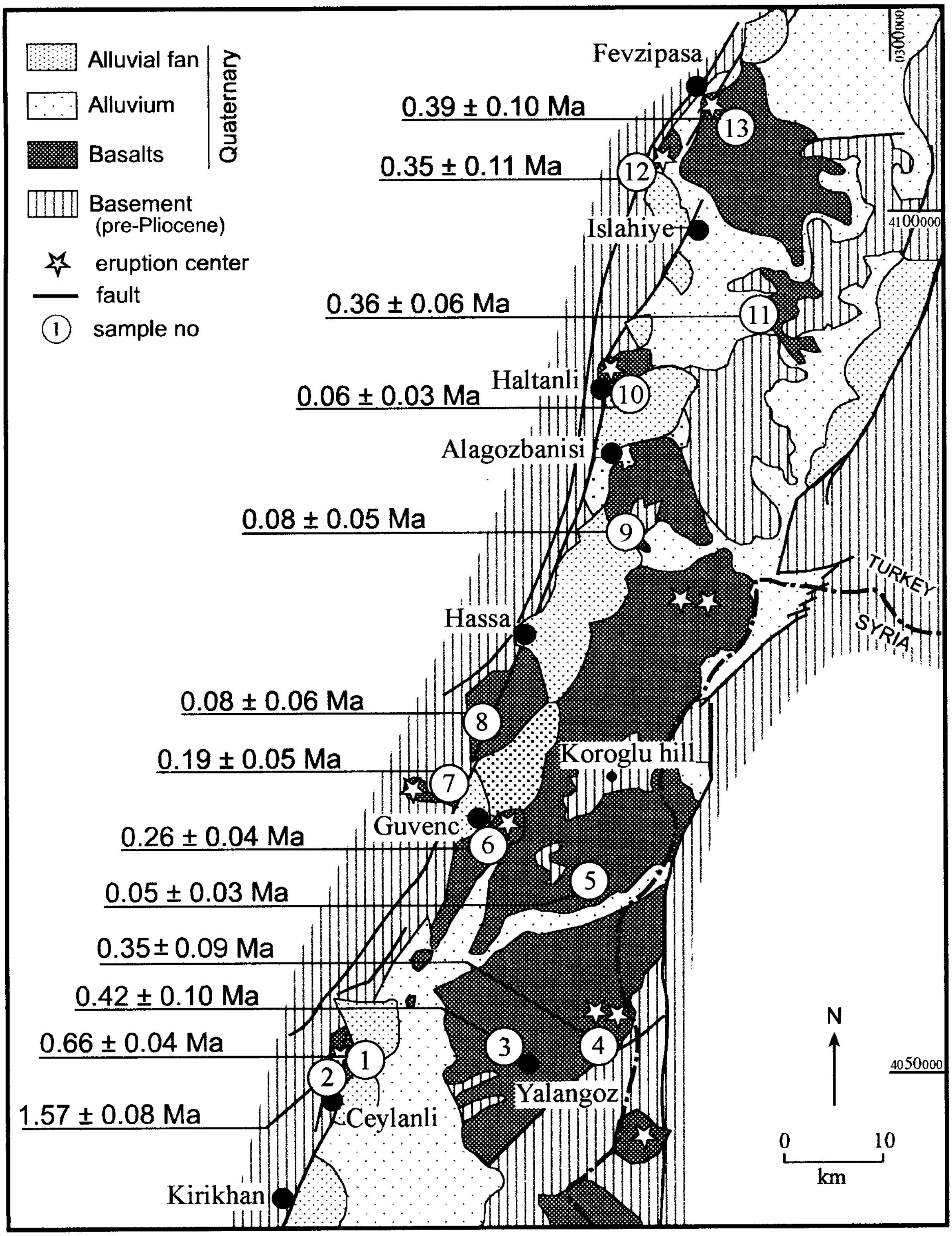

Figure 5. Distribution of Quaternary basaltic volcanics within the Karasu Rift and their K-Ar radiometric age datings.

Table III. Volcanic activity periods based on age and field relations.

Site No	Mean AgeandError(Ma)	Remarks
2	1.57 ± 0.08	Site is located on the rift shoulder. No exposed flows within the valley. Lavas are faulted. Therefore, the rift did not exist in its present shape.
		Time gap
1	0.66 ± 0.04	An eruption centre, which is located within the rift valley indicating the existence of the rift valley.
		Time gap
3	0.42 ± 0.10	
13	0.39 ± 0.10	Thick flows originated in the rift margins and flowed towards its centre.
11	0.36 ± 0.06	
12	0.35 ± 0.11	
4	0.35 ± 0.09	
		A possible time gap **(?)**
6	0.26 ± 0.04	
7	0.19 ± 0.05	Flows in river channels, which are at the present uplifted relatively to the present base level.
		A possible time gap **(?)**
8	0.08 ± 0.06	
9	0.08 ± 0.05	Flows within the rift valley that is in a morphological shape similar to the present. One flow (no.8) is faulted manifesting recent activity.
10	0.06 ± 0.03	
5	0.05 ± 0.03	

the marginal faults and therefore it seems that the valley at the time of the eruption did not have its present configuration. On the other hand, the 0.66 Ma sample comes from a volcano (Küçük Höyük), located inside the valley close to margins. Therefore, it seems that it was erupted at a time when the valley was already close to its present configuration. The absence of lava in borehole 475 suggests that these lavas do not have southern continuation beneath the alluvium (*table I*, *figure 4*).

Site 3 and 4 are from lavas located near Yalangöz and near the eastern margins of the valley (east of Yalangöz). These lavas, dated as 0.42 ± 0.10 Ma and 0.35 ± 0.09 respectively, come from one of the two eruption centres that are located close to the Turkish–Syrian border (*figure 5*). Nearby boreholes (no. 474, 2928, 2631) contain lavas alternating with subsurface Quaternary sediments (*table I*, *figure 4*).

Site 5, near Köroğlu hill (*figure 5*), is located in the southern part of the most widespread volcanic field of the area. Two eruption centres are located at the northern part of this field, close to the Turkish–Syrian border. This volcanic field and especially the dated lava, have a very fresh morphological appearance thus suggesting a young age. The radiometric dating yields an age of 0.05 ± 0.03 Ma that confirms the field data.

Site 6, dated to 0.26 ± 0.04 Ma, belongs to a volcanic unit having an eruption centre east of Güvenç (Aktepe) (*figure 5*). Field relations show that this lava is overlain by the lava of site 4, so the radiometric dating is concordant with the stratigraphy. Three lavas, with a thickness of 121 m, were drilled in borehole 472 and had a similar thickness at borehole 474. These two boreholes suggest an earlier volcanic field at the centre of the Karasu Rift.

Sites 7 (NW of Güvenç) and 8 (Hacılar, south of Hassa) are parts of lavas erupted from volcanic vents situated within a pre-existing Quaternary valley on the western margin of the rift (*figure 5*). The lavas, dated as 0.19 ± 0.05 and 0.08 ± 0.06 Ma respectively, flowed through the pre-existing stream valleys into the Karasu Rift. The front of both lavas was later faulted by the marginal faults. Hence, these faults have been active since 0.08 Ma.

Sites 9 (SE of Alagözbanısı) and 10 (NE of Haltanlı) were dated as 0.08 ± 0.05 and 0.06 ± 0.03 Ma, respectively. Petrographically both lavas were found to be very similar by our unpublished geochemical analyses as well as Çapan et al [33]. This and the age similarity suggest that the source of both lavas might be the same volcanic centre, which is probably located near Haltanlı along the western margin of the valley (*figure 5*). An alluvial fan now separates this volcanic field into two distinct parts.

Samples 11, 12 and 13 were collected from three separate volcanic fields in the Fevzipaşa–Islahiye area (*figure 5*). They were dated as 0.36 ± 0.06, 0.35 ± 0.11 and 0.39 ± 0.10 Ma, respectively. The field appearance as well as their age and petrographic similarity suggest that they were actually from the same volcanic field. The volcanic field extends a few kilometres to the north as it is evidenced by the presence of two lavas in borehole 14334 and by their absence in boreholes 14332 and 11294 (*table I*, *figure 4*). On the other hand, it seems that the volcanic fields, on which sites 10 (Haltanlı) and 11, 12, 13 (Fevzipaşa–Islahiye) were situated, are not

Table II. Radiometric dating of Karasu rift volcanics (see figure 5for site locations).

Site	Location	UTM-X Coor.	UTM-Y Coor.	Age (Ma)	Error (Ma-1σ)	LOI %(1)	%K	%^{40}Ar* (2)	^{40}Ar*(cc STP/gr) (x10^8)(3)	Meas. No.	Mean age and error (Ma)(4)	Çapan et al. (1987) (Ma)
				0.68	0.062		1.18	4.37	3.134	9352		
1	NE Ceylanlı	266945	4050285	0.67	0.025	0.9	1.18	13.03	3.074	9547	0.66 ± 0.04	
				0.62	0.038		1.18	20.75	2.851	9722		
				1.63	0.054		0.98	22.04	6.218	9560		
2	N Ceylanlı	265905	4049490	1.48	0.041		0.98	23.53	5.642	9737	1.57 ± 0.08	1.73 ± 0.10
				1.59	0.046		0.98	21.67	6.071	9344		
				0.34	0.041		1.05	11.07	1.396	9733		
3	NW Yalangöz	276705	4051190	0.52	0.037		1.05	10.69	2.110	9544	0.42 ± 0.10	0.78 ± 0.10
				0.41	0.077		1.05	2.69	1.677	9349		
				0.29	0.046		0.93	6.43	1.037	9347		
4	E Yalangöz	282600	4051050	0.45	0.040	0.2	0.93	10.65	1.622	9559	0.35 ± 0.09	
				0.32	0.022		0.93	8.87	1.153	9741		
5	S Köroğlu H.	281430	4060345	0.07	0.020		0.68	1.35	0.181	9549	0.05 ± 0.03	2.10 ± 0.20
				0.03	0.031		0.68	0.50	0.071	9350		
6	E Güvenç	276415	4064845	0.28	0.048		1.08	3.76	1.180	9351	0.26 ± 0.04	
				0.24	0.032		1.08	3.13	0.988	9545		
7	NW Güvenç	273835	4066305	0.19	0.046		0.91	4.32	0.665	9553	0.19 ± 0.05	0.60 ± 0.10
				0.13	0.065		0.94	1.41	0.460	9342		
8	S Hassa	275800	4070400	0.03	0.030		0.94	0.84	0.126	9743	0.08 ± 0.06	1.10 ± 0.20
				0.07	0.036		0.94	0.80	0.259	9546		
9	SE Alagözbanısı	285210	4081105	0.08	0.040		0.75	1.94	0.241	9548	0.08 ± 0.05	0.45 ± 0.15
				0.07	0.150		0.75	0.50	0.203	9341		
10	NE Haltanlı	283445	4084070	0.20	0.034		0.85	2.83	0.670	9555	0.06 ± 0.03	0.35 ± 0.15
				0.37	0.077		0.70	6.99	0.995	9561		
11	SE Islahiye	293065	4094825	0.41	0.088		0.70	5.13	1.111	9334	0.36 ± 0.06	
				0.31	0.048		0.70	6.47	0.854	9706		
				0.39	0.061		1.04	8.47	1.575	9562		
12	NW Islahiye	288455	4104695	0.22	0.018		1.04	10.29	0.888	9739	0.35 ± 0.11	1.17 ± 0.17
				0.44	0.054		1.04	3.02	1.798	9335		
				0.48	0.028		1.20	7.02	2.243	9563		
13	SE Fevzipaşa	290305	4107535	0.38	0.065	1.7	1.20	7.17	1.772	9343	0.39 ± 0.10	
				0.30	0.023		1.20	11.64	1.394	9745		

(1) LOI–Loss of mass on ignition
(2) Percent of the radiogenic argon.
(3) CC STP per gram of radiogenic ^{40}Argon
(4) Uncertainties on a single measurement were calculated using the Gauss method as described by Heimann (1990). Mean uncertainties from multiple samples at a single site were derived using a formulation taking into account the uncertainty of each individual determination and the dispersion of ages of multiple samples of each site. This approach results in a larger uncertainty than would be implied by a single standard deviation on all the ages, and probably represents the actual uncertainties better than less conservative estimates.

connected to each other as no lavas were indicated in borehole 15198. This is also supported by the significant age differences (0.36 vs. 0.07 Ma).

To summarize: the Quaternary volcanic field of the Karasu Rift is located between Fevzipaşa and the north of Reyhanlı, which are the north and northeastern parts of the valley. The Quaternary basaltic volcanism was dated in this study to 1.6 to 0.05 Ma which is much younger than the ages (2.10 to 0.35 Ma) previously proposed by Çapan et al [33].

The lavas are differentiated into five groups considering their ages and the field relations (*table III*). There are two clear time gaps within the Quaternary volcanic activity between 1.57 ± 0.08 Ma and 0.66 ± 0.04 Ma, and between 0.66 ± 0.04 Ma and 0.42 ± 0.10 Ma. Other two possible time gaps can also be present between 0.35 ± 0.11 Ma and 0.26 ± 0.04 Ma, and between 0.19 ± 0.05 Ma and 0.08 ± 0.06 Ma. The age relations indicate intermittent volcanism within the Karasu Rift.

4. Quaternary basin fill

The Plio-Quaternary Karasu valley is filled with fluvial and lacustrine sediments interfingered and covered with the volcanic sequence (*figure 3*). Although these two rock groups are intercalated in some parts of the area, in general, they are observed in different parts of the rift. Recent alluvium, alluvial fans, talus, and lake deposits dissect the Plio-Quaternary sediments. Accumulations of travertine and caliche-like deposits are present in Antakya and north of Kırıkhan along the western margin of the valley.

The nature and the thickness of sedimentary fill vary from the margins to the centre of the valley. Along the margins, alluvial fans and talus deposits, which are composed of coarse-grained clastics, reach 220 m thickness, unconformably overlying basement rocks. On the other hand, the basinal units are pre-dominantly light coloured clayey clastics of up to 465 m thickness, with minor lenses of conglomerate.

Distribution of the sedimentary fill in the rift was investigated using borehole data provided from State Hydraulic Works (Devlet Su İşleri, DSİ) [42] (*table I*, *figure 4*).

The sedimentary facies and thickness of the sequence varies locally in different parts of the valley. The sediment fill has a considerable thickness in the area between Fevzipaşa and the Amik Lake, particularly along the western margins of the valley. The maximum observable thickness on the western margin of the valley is more than 362 m (borehole 477, *figure 4*). This borehole was drilled through coarse clastic sediments but did not reach the basement.

Within the Amik Plain the deposits gradually thickens from the margins towards the centre. The maximum thickness of the Quaternary fill is more than 350 m according to DSİ wells (*table I*, boreholes 2929,479) and more than 465 m according to TPAO (Turkish Petroleum Company) research wells [32]. However, sudden changes in the thickness are observed in closely spaced boreholes in adjacent localities having almost the same altitude. For example, the thickness is 70 m in borehole 1273 but just south the thickness is more than 350 m (borehole 2929). A similar variation can be observed between boreholes 481 and 2630. This phenomenon may indicate buried faults with significant vertical displacements in the Quaternary sequence.

The Quaternary sedimentary sequence intercalates in several boreholes with basaltic lavas, as is also observed at the surface (*table I*).

5. Pattern of faults

The major faults are typically parallel to the NNE trend of the Karasu valley (*figure 2*). Field mapping was carried out using satellite images, aerial photographs, and previous maps [20, 22, 23, 31–33].

The faults affecting the Karasu Rift and its surrounding can be divided into four groups based on their spatial distribution and their patterns from rose diagrams (*figures 3* and *6*). (1) the western margin faults, (2) the eastern margin faults, (3) the southern margin faults, and (4) faults between Antakya and Samandağ. Weighted rose diagrams of these faults are presented, to illustrate their statistical distribution (*figure 6*).

5.1. The Western margin faults

The faults at the western margin of the Karasu Rift strike NNE. From Fevzipaşa to Kırıkhan, they form a zone that trends N10°–50°E (*figure 6A*). The principle faults in this wide zone are oriented towards N17°–24°E. Other concentrations correspond to secondary faults. The major faults generally dip between 65°and 90° to the east and display left-lateral oblique-slip faulting.

The relationship between the main fracture and the secondary faults displays a left-stepping (from Fevzipaşa in the north to Antakya in the south) and fanning out (from Fevzipaşa in the north to Kırıkhan in the south) patterns which result in the development of several small scale pull-apart basins (*figure 3*).

It should be mentioned that many eruption centres are located along the western margin faults of the Karasu Rift. One volcano located in the north of Kırıkhan, two in the south of Hassa, one in the south of Islahiye and two in the south of Fevzipaşa are examples for these eruption centres (*figure 5*).

5.2. Eastern margin faults

The eastern margin faults of the Karasu Rift strike mainly NNE, generally parallel to the western margin faults. The

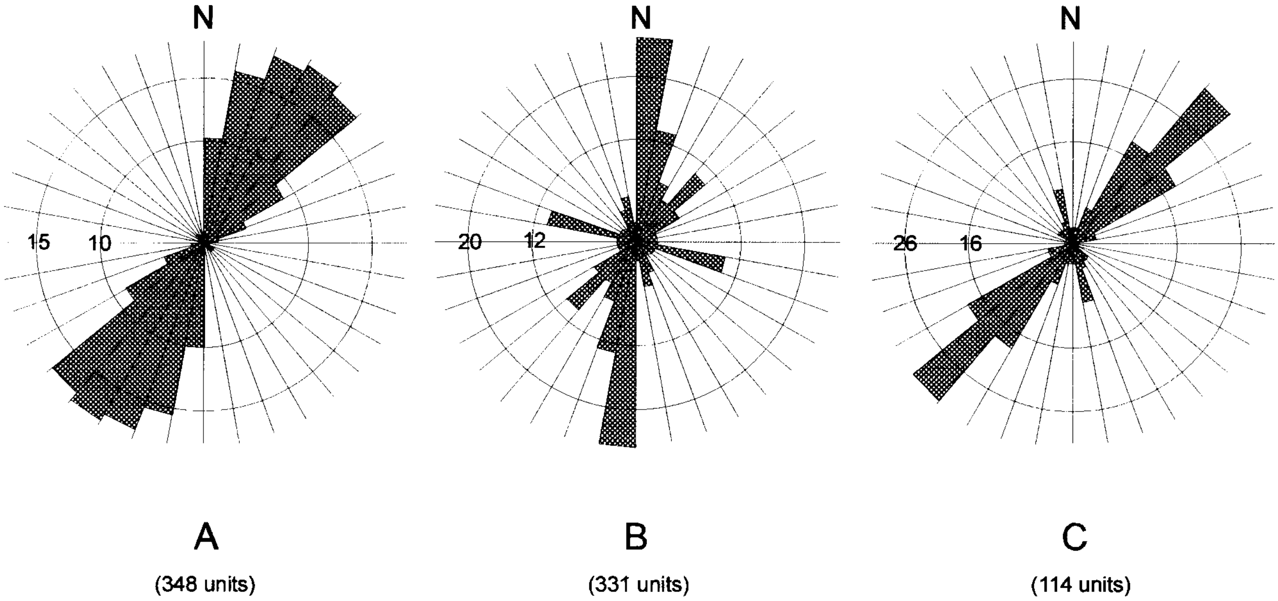

Figure 6. Weighted rose diagrams of A) western margin (Fevzipaşa to far south of Kırıkhan), B) eastern and southern margins, C) Antakya–Samandağ faults.

main trend of this fault system is N00°–20°E (*figure 6B*), which corresponds to the main fault system from the Asi River valley (south of Amik Plain) to Hassa in the north. These are left-lateral strike-slip faults with only minor components of normal-slip [28] (*figure 3*). These faults have steeper scarps, with less frequent and smaller alluvial fans and combined talus deposits than the western margin faults. The Asi River fault system display elevated blocks on the eastern side (Syrian side) relative to the western blocks (Turkish side) where the Asi River flows parallel to the faults. Small-scale, almost N–S-trending horsts and grabens are identified on Syrian side by aerial photographic studies (*figure 3*). The relationship between these faults and the basin fill suggests that these faults have been active during the Late Quaternary. A few small-scale faults form the northern continuation of the eastern margin faults to the northeast of Hassa, which bend slightly eastward into a direction of N20°–30°E.

Other faults display a typical trend between N40°–50°E (*figure 6B*), which reflect the main trend of secondary faults along the eastern margins. Most of these faults are on the Syrian side and were mapped from aerial photographs (*figure 3*).

5.3. Southern margin faults

The southern margin of the Karasu Rift is bounded by a geomorphologically less impressive fault system. These faults have an almost perpendicular strike (N70°–80°W) to the main trend of the fault systems of the Karasu Rift (*figures 3* and *6B*). The southern margin faults are right-lateral oblique-slip faults with the northern block (Amik Plain side) downthrown [28]. Three of these faults bound the southern margin of the Amik Plain, extrending from the western margin of the rift to far southeast of Reyhanlı [22] (*figure 3*).

5.4. Antakya–Samandağ faults

The southern tip of the western margin faults bend from N20°E (Fevzipaşa–Kırıkhan trend) to N38°–47°E trend (SW of Kırıkhan–Samandağ) at the western margins of the Amik Plain (*figure 3*). This bending and left step-over of the fault system resulted in the development of the N38°E-trending Antakya–Samandağ depression (*figure 3*). The faults within this system display a left-lateral oblique slip faulting to normal faulting from southwest of Kırıkhan to Antakya–Samandağ.

Two concentrations of faults are observed in the Antakya–Samandağ depression. The dominant one has normal faulting with left-lateral strike-slip component, with a wide range of strike (N30°–60°E) and the second concentration has right-lateral strike-slip faulting in a trend of N10°–20°W (*figure 6C*).

During the course of the present study a total of 26 slip lineation data were measured in four sites along different segments of the major faults between Antakya and Kırıkhan (*figure 3*). Three of these sites are located along the faults displacing Pliocene units and one displacing pre-Pliocene basement and controlling the evolution of Quaternary deposition.

The first site is from the faults southwest of Antakya (UTM coordinates; 2 43 500 – 40 07 700) bordering the Antakya–Samandağ depression from south (*figure 3*). The faults have developed in Neogene limestones and have an attitude of N 42°–66°E/ 66°N with rake of 72°S.

The second site is from north of Antakya (UTM coordinates; 2 46 900 – 40 21 400) on N30°E/69°S dipping faults with a rake of 34°S. These developed on Neogene clastics bordering the Antakya–Samandağ depression to the north (*figure 3*).

The third site is north of Antakya (UTM coordinates; 2 47 900 – 40 24 400) on various faults having different orientations and senses. One group is of N 20°–47°E/ 66°S dipping faults with 45°N rake. A second one is a N56°E/ 54°S dipping fault with pure dip slip. The third is from a N47°W/ 85°N dipping fault with a 36°N rake. The last is from a N46°W/ 82°S fault with a 56°S rake (*figure 3*).

The fourth site is from west of Kırıkhan (UTM coordinates; 2 54 050 – 40 40 600) on a N30°–42°E/ 70°S fault with 76°S rake. This fault is developed between Neogene clastics and pre-Neogene basement rock units (*figure 3*).

Four dominant sets of faults are detected from these measurements with NE–SW strike. The faults dip in two dominant sets of NW and SE directions. The rake amount ranges from 34° to 76° suggesting a normal oblique-slip faulting with left-lateral components along the Antakya–Samandağ depression.

6. Neotectonic characteristics of the Karasu Rift

6.1. Geomorphologic Features

The Karasu Rift is a well-recognised depression bounded by highly elevated shoulders. The Amik depression, located at the southern part of the Karasu Rift at an altitude of 82 m, is to the widest and deepest part of the rift, and is its main depocenter (*figure 3*). The major rivers (Karasu, Afrin and Asi) flow to the centre of this basin (Amik Lake), which is drained by the Asi River into the Mediterranean Sea at Samandağ (*figure 3*).

The eastern and western margins of the rift display morphological differences. The western margin of the rift (the Amanos Mountains) is uplifted to a height of up to 2 250 m. Maximum morphological relief difference of the valley is more than 2 000 m. The eastern margin, on the other hand, has relatively low topography where its maximum height is 800 m. This geomorphological asymmetry reflects the asymmetric evolution of the rift valley.

The western margin is ornamented with a series of extensive, aligned, combined, thick alluvial fans, particularly between Antakya and Fevzipaşa (*figure 3*). Slopes of these alluvial fans range from 0.4° to 2°, with a radius of 2.7 to 4.5 km. However, there are smaller, more recent fans with steeper slopes of up to 4°. Most of these fans are circular, with almost no internal deformation and dissection, except the fans in the vicinity of Kırıkhan and Hassa that are cut, offset and elongated by recent faulting.

The individual, en-echelon, bifurcating and braided fault patterns (*figures 2* and *3*) gave rise to the development of various young geomorphologic structures. Step-like morphology is a common feature along the rift margins due to the overlapping of faults. These features are observed particularly along the western margins, on both sides of the Antakya–Samandağ and Asi River valleys (*figure 3*). Elongated ridges and depressions are aligned parallel to the NNE–SSW-striking faults and are observed especially along the western margin. Long narrow morphotectonic depressions that are small-scale pull-aparts are located along the western margin of the valley between en-echelon left-lateral strike-slip faults. On the other hand, the eastern margins are mainly controlled by the N–S-striking straight faults along which the eastern blocks are uplifted (*figure 3*). Thus, it seems that the present geomorphology of the Karasu Rift is controlled by its neotectonic activity.

6.2. Young displacements along faults – amount and rate

There is no direct evidence for vertical or horizontal displacement along the Karasu faults. The diverted stream channels displaced lavas and elevated terrace conglomerates are the only indicators of displacements observed during this study.

The sense of displacement along the faults, and in some places also its amount, can be detected in several cases in the alluvium, alluvial fans, volcanic units and by recognising diverted stream channels. Most of the stream channels are generally left-laterally diverted and/or diminished along the fault lines indicating a sinistral motion along the faults of Karasu Rift during the latest Quaternary period

The amounts of horizontal offset of the streams range between 50 and 675 m throughout the zone. In most cases the streams flow almost perpendicular to the faults and therefore the stream offset is most probably equivalent to the strike-slip component of faulting.

The recorded oldest age of faulting is directly deduced from radiometric age of the displaced volcanic rocks. South of Hacılar Village, a basaltic lava (*figures 3*and *5*, site 7) is displaced vertically (55 m) and laterally (325 m) where the lava was dated as 0.08 ± 0.06 Ma (*table II*). Therefore, the minimum horizontal rate of displacement is 4.06 mm·year^{-1} while the vertical rate of displacement is at least 0.69 mm·year^{-1}. Accordingly, the rate of the net slip is at least 4.1 mm·year^{-1} along this fault since 80 000 BP.

It should be noted that along the Karasu Rift no compressive structures are found belonging to the Quaternary period. However, to the north of the rift along the EAFZ, Quaternary overthrusts are recognised [23, 27, 43]. Westaway and Arger [24] and Yürür and Chorowicz [28] suggested that these structures are formed in a phase of N–S directed compression and were later displaced by the young activity of the EAFZ.

7. Discussion

The Karasu Rift has developed as a result of N–S convergence of the Eurasia and Arabian plates, and the westward escape of the Anatolian Plate and the Amanos Mountains sector. The geological processes that characterise the Plio-Quaternary evolution of the Karasu Rift are the contemporaneous volcanism, sedimentation and faulting.

Quaternary basaltic volcanism that was derived from metasomatised asthenospheric or lithospheric mantle is most probably related to syn-collisional transtensional strike-slip deformation in the Karasu Rift [eg., 38]. This is due to decompressional partial melting as the overlying continental lithosphere was stretched, thinned and ruptured by the EAFZ and DST [28, 38]. The Quaternary volcanism of the Karasu Rift may have reached the earth's surface more easily along the Karasu Rift faults that are most probably following pre-existing crustal lineaments [28, 33, 38]. However, the origin of these intra-plate basalts is still the subject of debate [e.g., 44].

The volcanism of the Karasu Rift was previously identified as olivine tholeiites to quartz tholeiites and alkali olivine basalts, from older to younger, respectively [28, 33, 38, 39]. However, our investigations suggest that the stratigraphic order of the volcanics is different to what has been previously proposed. For example, our results suggest that the alkali olivine basalts at Ceylanlı (N of Kırıkhan) are the oldest and the olivine tholeiites in the Köroğlu hills are the youngest volcanics in the Karasu Rift (*figure 5*, *table II*). Previously however, the alkali olivine basalts have been presumed to be the youngest volcanics within the valley and the olivine tholeiites to be the oldest.

There is a clear time gap between this volcanism and the Neogene volcanism in the region around Maraş [eg., 39]. There is indeed no recorded Neogene volcanism within the Karasu Rift [33, 38, 39]. The volcanic activity in the Karasu Rift during the Quaternary has been intermittent. Two clear time gaps are present between 1.57 ± 0.08 Ma and 0.66 ± 0.04 Ma, and between 0.66 ± 0.04 Ma and 0.42 ± 0.10 Ma (*table III*).

Radiometric dating of the Quaternary volcanics of the Karasu Rift was previously in an age span of 2.10 to 0.35 Ma [33]. However, there are considerable differences between radiometric dates of the present study and previous studies (*table II*) [33, 39]. We obtain 0.35 ± 0.11 Ma for the same tholeiitic lava, sampled from the same locality (S of Fevzipaşa) by Çapan et al [33], which was 1.17 ± 0.11 Ma old (Sample 12 in *table II*). Another example is the clear difference between Yalangöz and Köroğlu volcanics. The Köroğlu volcanics are stratigraphically younger than the Yalangöz volcanics. This is observed in the field, and led us to sample the same localities that Çapan et al [33] sampled. This field observation was later well reflected by our radiometric dating of these volcanics. Our ages for the Yalangöz volcanics range from 0.42 ± 0.10 to 0.35 ± 0.09 Ma and 0.05 ± 0.03 Ma for the Köroğlu volcanics. However, these volcanics were considered to be the same unit and were assigned an age of 2.10 ± 0.20 to 0.78 ± 0.10 Ma by Çapan et al [33].

The Karasu fault zone has experienced relatively recent displacements as clearly manifested by offset of Quaternary basalts. A lava flow, dated as 0.08 ± 0.06 Ma, is displaced vertically by 55 m and left-laterally by 325 m, indicating a left-lateral oblique-slip movement (*figures 3*and *5*). Therefore, the minimum horizontal rate of displacement is 4.06 mm·year^{-1} while the vertical rate of displacement is at least 0.69 mm·year^{-1}. Accordingly, the rate of the net slip is most probably at least 4.1 mm·year^{-1} along this fault since 80 000 years. This slip rate is smaller than most of the previous proposed slip rates for the EAFZ (4–10 mm·year^{-1} by Kuran [45]; 9 mm·year^{-1} by Kasapoğlu [46]; 7.8–9 mm·year^{-1} by Yürür and Chorowicz [28]; 29 mm·year^{-1} by Taymaz et al [26]; 19 mm·year^{-1} by Lyberis et al [23]; 6 mm·year^{-1} by Kiratzi [47], 6 mm·year^{-1} by Westaway and Arger [24]) and for the DST (6–8 mm·year^{-1} by Garfunkel [48]; 11 mm·year^{-1} by Kasapoğlu [46]; and Westaway [27]); for Gharb segment of DST (4 to 5 mm·year^{-1} by Westaway and Argar [24]). This wide range of slip rate is basically computed from various kinematic models and/or seismic data. Our slip rate, 4.1 mm·year^{-1}, is only for the Karasu fault zone that links Gharb segment of DST and EAFZ, and from a displaced 80 000-year-old lava.

A comprehensive slip lineation analysis of fault surfaces [28] concluded that two phases of deformation occurred at the area; older N–S directed compressional phase and a more recent E–W extensional phase. However, we could not observe any overprinting on fault surfaces in Antakya–

Kırıkhan sector. During the present study 26 slip lineation data were measured where fault bends from N20°E (Fevzipaşa–Kırıkhan trend) to N38°–47°E direction (Kırıkhan–Samandağ trend). The faults have NE–SW strike with a rake of 34° to 76° suggesting a normal oblique-slip faulting with left-lateral components. The normal component of faulting increases from north (left-lateral strike-slip faulting with normal component, SE of Hassa) to south (normal faulting with left-lateral strike-slip component, around Antakya). This releasing bend gave rise to the development of the Antakya–Samandağ depression, where no neotectonic compressional components are recorded [23].

8. Conclusions

The results of the present study revealed the structure of the NNE-trending Karasu fault zone that binds the Karasu Rift to the west and form the Karasu Rift itself.

The NNE-trending Karasu fault zone acts as a linkage zone between left-lateral transform faults, namely, the N–S-trending Gharb segment of the DST and the NE-trending EAFZ. The northern end of the fault zone intersects the EAFZ south of Maraş whereas its southern end splays out into N30°E-trending Antakya–Samandağ fault segment and N–S-trending Asi River fault segment.

The rift is developed between east dipping NNE-striking faults of Karasu fault zone which defines the western margin of the rift, and the west dipping N–S to NNE–SSW-striking faults of DST which control the central part and eastern margin of the rift. The bend from N20°E to N47°E gave rise to the development of a releasing area where the Antakya–Samandağ depression developed and an asymmetrical widening of the Karasu Rift occurred during the Quaternary period. The faults within this zone display normal faulting with a left-lateral component.

The asymmetry of the rift is reflected by a series of extensive, combined, thick alluvial fans aligned on western margin and topographically elevated western rift shoulders relative to eastern margin.

Quaternary fluvial to lacustrine sedimentation within the rift is contemporaneous with alkali basaltic volcanism between 1.57 ± 0.08 Ma and 0.05 ± 0.03 Ma. This is displayed by the intercalation of Quaternary fluvial deposits with basaltic volcanics in borehole data. In eleven boreholes out of thirty-one [42], Quaternary basaltic volcanics and fluvial deposits are intercalated (*table I*). In three boreholes (no. 472, 479 and 2632), three basaltic flow units are encountered with a maximum total thickness of 121 m (borehole no. 472) (*table I*). On the other hand, the maximum thickness of Quaternary sedimentary fill is 350 m (borehole no. 2929) [42].

The Quaternary volcanic field of the Karasu Rift is located between Fevzipaşa and north of Reyhanlı. Field and borehole data suggest that this volcanism is limited in spatial distribution and by volume. The limits, northeast of Fevzipaşa, and north of Amik Lake, of the volcanic field are estimated by the presence or absence of the basaltic lavas in boreholes and in the field.

Thirteen new K-Ar dates for the Karasu Rift volcanism are provided. The age of the alkali basaltic volcanism of the Karasu Rift determined in present study (1.57 ± 0.08 to 0.05 ± 0.03 Ma) is systematically much younger than the previous age determinations in the same region (2.10 to 0.35 Ma) by Çapan et al [33].

The lava flows are grouped into five phases by their ages and field relations (*table III*). This illustrates intermittent volcanic activity within the Karasu Rift.

The sense of slip along the faults, and in some cases also its amount, can be detected in many cases in the displaced volcanic units, elevated terrace conglomerates and diverted stream channels. Our K-Ar dates do provide new constraints on fault slip rates. The rate of left-lateral slip is calculated approximately as 4.1 mm·year^{-1} from displaced lavas which are 80 000 years old.

Overall, the Karasu fault zone is a linkage zone between DST and EAFZ where basaltic volcanism has accompanied the faulting between 1.57 ± 0.08 and 0.05 ± 0.03 Ma.

Acknowledgements. The authors are grateful to The Scientific and Research Council of Turkey (TÜBİTAK) and Israel Geological Survey for their financial support during field and laboratory studies with a Research Fund Project. We would like to thank Erdin Bozkurt for his patience and encouragement. And finally we would like to express our special thanks to Rob Westaway and Aykut Barka for their comments that greatly improved an earlier version of this manuscript.

References

[1] McKenzie D.P., Active tectonics of the Mediterranean region, Geophys. J.R. Astr. Soc. 30 (1972) 109–185.

[2] Sengör A.M.C., Yılmaz Y., Tethyan evolution of Turkey: a plate tectonic approach, Tectonophysics 75 (1981) 181–241.

[3] Dewey J.F., Hempton M.R., Kidd W.S.F., Saroglu F., Şengör A.M.C., Shortening of continental lithosphere: the neotectonic of Eastern Anatolia – a young collision zone, in: Coward M.P., Ries A.C. (Eds.), Collision Tectonics, 19, Geolological Society Special Publication, London, 1986, pp. 3–36.

[4] Hempton M.R., Constraints on Arabian plate motion and extensional history of the Red Sea, Tectonics 6 (1987) 687–705.

[5] Le Pichon X., Gaulier J.M., The rotation of Arabia and the Levant fault system, Tectonophysics 153 (1988) 271–294.

[6] Şengör A.M.C., Türkiye'nin neotektoniğinin esasları, Geol. Soc.Turkey Conf. Ser. 2, 1980, 40 p.

[7] Le Pichon X., Angelier J., The Hellenic arc and trench system: a key to the neotectonic evolution of the eastern Mediterranean Sea, Tectonophysics 60 (1979) 1–42.

[8] Şengör A.M.C., Görür N., Saroğlu F., Strike slip faulting and related basin formation in zones of tectonic escape: Turkey as a case study, Soc. Econ. Paleontol. Mineral. Spec. Publ. 37 (1985) 227–264.

[9] Mart Y., Rabinowitz P.D., The northern Red Sea and the Dead Sea Rift, Tectonophysics 124 (1986) 85–113.

[10] Joffe S., Garfunkel Z., Plate kinematics of the cırcum Red Sea – a re-evaluation, Tectonophysics 141 (1987) 5–22.

[11] Quennell A.M., The structural and geomorphic evolution of the Dead Sea rift, Q. J. Geol. Soc. London 114 (1958) 1–24.

[12] Quennell A.M., Tectonics of the Dead SeaRift. 20th Int. Geol. Congr., Mexico 1956, 1959, pp. 385–405.

[13] Freund R., Garfunkel Z., Zak I., Goldberg M., Weissbrod T., Berin B., The shear along the Dead Sea rift, Phil. Trans. Roy. Soc., London, Serie A 267 (1970) 107–130.

[14] Garfunkel Z., Zak I., Freund R., Active faulting in the Dead Sea rift, Tectonophysics 80 (1981) 1–26.

[15] Freund R., Zak I., Garfunkel Z., On the age and rate of sinistral movement along the Dead Sea rift, Nature 220 (1968) 253–255.

[16] Dubertet L., Liban, Syrie et Bordure des pays voisins. Extrait des notes et mémoires sur le moyen-orient, tome VIII. Museum national d'histoire naturelle, 1966, 251–358.

[17] Chaimoy T.A., Barazang M., Crustal shortening in the Palmyride Fold Belt, Syria, and implications for movement along Dead Sea fault system, Tectonics 9 (1990) 1369–1386.

[18] Arpat E., Şaroğlu F., The East, Anatolian fault system: thoughts on its development, Bull. Min. Res. Expl. Inst. Turkey 78 (1972) 33–39.

[19] Seymen İ., Aydın A., Bingöl deprem fayi ve bunun Kuzey Anadolu fayı ile ilişkisi, Bull. Min. Res. Expl. Inst. Turkey 79 (1972) 1–8.

[20] Muehlberger R.W., The splintering of the Dead Sea fault zone in Turkey, Hacettepe Univ. Earth Sci. 8 (1981) 123–130.

[21] Jackson J., McKenzie D., Active tectonics of the Alpine–Himalayan Belt between Western Turkey and Pakistan, Geoph. J. R. Astr. Soc. 7 (1984) 185–264.

[22] Şaroğlu F., Emre Ö., Kusçu İ., The East Anatolian fault zone of Turkey, Annales Tectonicae 6 (1992) 99–125.

[23] Lyberis N., Yürür T., Chorowicz J., Kasapoğlu E., Gündoğdu N., The East Anatolian fault: an oblique collisional belt, Tectonophysics 204 (1992) 1–15.

[24] Westaway R., Arger J., The Gölbaşı basin, southeastern Turkey: a complex discontinuity in a major strike-slip fault zone, J. Geol. Soc. London 153 (1996) 729–744.

[25] Eyidoğan H., Bitlis-Zagros Bindirme Kusaginin Sismotektonik Özellikleri, PhD thesis, İstanbul Tech. Univ. Fac. Mining, İstanbul, 1983.

[26] Taymaz T., Eyidoğan H., Jackson J., Source parameters of large earthquakes in the East Anatolian Fault Zone (Turkey), Geophys. J. Int. 106 (1991) 537–550.

[27] Westaway R., Present day kinematics of the Middle East and Eastern Mediterranean, J. Geophys. Res. 99 (1994) 12071–12090.

[28] Yürür T., Chorowicz J., Recent volcanism, tectonics and plate kinematics near the junction of the African, Arabian and Anatolian plates in the eastern Mediterranean, J. Volcan. Geother. Res. 85 (1998) 1–15.

[29] Perinçek D., Çemen İ., The structural relationship between the East Anatolian and Dead Sea fault zones in Southeastern Turkey, Tectonophysics 172 (1990) 331–340.

[30] Gülen L., Barka A., Toksöz M.N., Continental collision and related complex deformation: Maraş triple junction and surrounding structures, SE Turkey, Hacettepe Univ. Earth Sci. 14 (1987) 319–336.

[31] Muehlberger R.W., Gorbon M.B., Observations on the complexity of the East Anatolian Fault, Turkey, J. Struct. Geol. 9 (1987) 899–903.

[32] Perinçek D., Eren A.G., Doğrultu atımlı Doğu Anadolu ve Ölü Deniz fay zonları etki alanında gelişen Amik havzasının kökeni, Türkiye 8. Petrol Kongresi Bildiri Kitabi, 1990, 180–192.

[33] Çapan U.Z., Vidal P., Cantagrel J.M., K-Ar, Nd, Sr and Pb Isotopic study of the Quaternary volcanism in Karasu Rift (Hatay), N-end of Dead sea rift zone in SE Turkey, Hacettepe Univ. Earth Sci. 14 (1987) 165–178.

[34] Lovelock P.E.R., A review of the tectonics of the northern Middle East region, Geological Magazine 121 (1984) 577–587.

[35] Ergin K., Guclu U., Uz Z., A catalogue of earthquakes for Turkey and surrounding area (11A.D. to 1964 A.D.). İstanbul Tech. Univ. Fac. Mining Publ., 24, 1967.

[36] Erdik M., Aydınoğlu N., PınarA., Kalafat D., Hatay Deprem Raporu Kandilli Obs., İstanbul, 1997.

[37] Tekeli O., Erendil M., Whitechurch H., Autochthons, parautochtons and ophiolites of the Eastern Taurus and Amanos mountains 1983, Field guidebook, PUBLISHER, LOCATION, 1983.

[38] Polat A., Kerrich R., Casey J.F., Geochemistry of Quaternary basalts erupted along the East Anatolian and Dead Sea fault zones of Southern Turkey: implications for mantle sources, Lithos 40 (1997) 55–68.

[39] Arger J., Mitchell J., Westaway R.W.C., Neogene and Quaternary volcanism of southeastern Turkey, in: Bozkurt E., Winchester J.A., Piper J.D.A. (Eds.), Tectonics and Magmatism in Turkey and the Surrounding Area, 173, Geolological Society Special Publication, London, 2000, pp. 459–487.

[40] Heimann A., The development of the Dead Sea Rift and its margins in northern Israel during the Pliocene and the Pleistocene. Ph.D. Thesis (in Hebrew with English abstract), The Hebrew University, Jerusalem, 1990.

[41] Heimann A., Ron H., Geometrical changes of plate boundaries along part of the northern Dead Sea transform: geochronology and palaeomagnetic evidence, Tectonics 12 (1993) 477–491.

[42] DSİ Report, Asi havzası hidrojeolojik etüt raporu, 1975.

[43] Karig D.E., Kozlu H., Late, Palaeogene evolution of the triple junction region near Maraş, south-central Turkey, J. Geol. Soc. London 147 (1990) 1023–1034.

[44] McKenzie D.P., O'Nions R.K., The source regions of ocean island basalts, J. Petrol. 36 (1995) 133–159.

[45] Kuran U., The location, magnitude and long-term time prediction of damaging earthquakes along the Anatolian faults and Levant coast, Bull. Geo. Congress of Turkey 2 (1980) 151–163.

[46] Kasapoğlu E.K., Seismotectonic characteristics of Eastern Mediterranean: A finite elements analysis, Hacettepe Univ. Earth Sci. 14 (1987) 309–317.

[47] Kiratzi A.A., A study of the active crustal deformation of the North and East Anatolian fault zones, Tectonophysics 225 (1993) 191–203.

[48] Garfunkel Z., Internal structure of the Dead Sea leaky transform (rift) in relation to plate kinematics, Tectonophysics 80 (1981) 81–108.

[49] Barka A., Reilinger R., Active tectonics of the Mediterranean region: deduced from GPS, neotectonic and seismicity data, Annali Geoph. 11 (3) (1997) 587–610.

[50] Mascle J., Chaumillon E., Pre-collisional geodynamics of the Mediterranean Sea: the Mediterranean Ridge and the Tyrrhenian Sea, Annali Geoph. 11 (3) (1997) 569–586.

[51] Mantovani E., Albarello D., Tamburelli C., Babbucci D., Viti M., Plate convergence, crustal delimination, extrusion tectonics and minimization of shortening work as main controlling factors of the recent Mediterranean deformation pattern, Annali Geoph. 11 (3) (1997) 611–643.

[52] Tolun N., Pamir H.N., Hatay. 1:500 000 ölçekli Türkiye jeoloji haritasi, M.T.A. Ankara, 1975.